SDC-92-187

SDC
SOLENOIDAL DETECTOR NOTES

ON THE "MASSLESS GAP" ADJUSTMENT OF DETECTED ENERGY FOR PASSIVE MATERIAL IN FRONT OF A CALORIMETER

Hans-Jochen Trost
Argonne National Laboratory

January 31, 1992

The submitted manuscript has been authored by a contractor of the U. S. Government under contract No. W-31-109-ENG-38. Accordingly, the U. S. Government retains a nonexclusive, royalty-free license to publish or reproduce the published form of this contribution, or allow others to do so, for U. S. Government purposes.

ANL/HEP/TR-92/06
SDC-92-187

On the "massless gap" adjustment of detected energy for passive material in front of a calorimeter*

HANS-JOCHEN TROST

High Energy Physics Division - 362 -
Argonne National Laboratory
9700 S. Cass Ave., Argonne, IL 60439-4815, USA

31 January 1992

ABSTRACT

I have designed a correction scheme for energy losses in passive material in front of a calorimeter based on the "massless gap" idea. I use a flexible geometry model of a calorimeter design for SDC outside of a solenoidal coil made of aluminium cylinders of adjustable thickness. The signal from the first radiation length of active calorimetry is scaled dependent on the incoming and observed energies of the shower. A reasonable recovery of the resolution of an unobstructed calorimeter is achieved using correction factors that depend only upon the total thickness of passive material. Thus a useful correction may be built into the hardware by increasing the amount of scintillator in the first radiation length of the active calorimeter. The distribution of correction factors determined event-by-event indicate that an additional dependence on the observed signal in the massless gap and total incident energy is clearly present.

* Work supported by the U.S. Department of Energy, Division of High Energy Physics, Contract W-31-109-ENG-38

1. Introduction

The accurate measurement of particle and jet energies is one of the central performance goals for designing and constructing the SDC detector.[1] A recurring issue in this context is the amount of material in front of the active calorimetry.[2–5] One method to accomodate passive material is to install "massless gaps",[2,6–9] *i.e.* some active element, into or just behind the passive material to turn it into a more or less small sampling calorimeter on its own. With the solenoidal coil and tracking systems in front, the SDC calorimeter[1] has to cope with this kind of a problem to some degree. I have chosen to use the ANLSIM simulation program[10] with the a flexible geometry model[11] to design and test a correction scheme of the massless gap variety for relatively localized passive material, like the solenoidal coil and calorimeter shell materials, in front of the calorimeter for showers from single electrons at energies of 10, 20, and 50 GeV.

2. Detector setup and analysis method

The detector model used in the present study has been described in detail before.[5] For my present purpose, I point single particle beams at 90° into the barrel calorimeter (Fig.1) and vary the thickness of the central cylinder in the coil model to obtain the desired round amounts of passive material (1, 2, 3 and 5 radiation lengths). In the program, the calorimeter is represented by a material mixture appropriate for a sandwiching of 4 mm thick lead absorbers and 4 mm thick scintillator tiles through the full depth of the calorimeter, with no additions for air gaps, wrappings, readout cracks or any mechanical support members. To calibrate the calorimeter response, I also made runs without any coil, *i.e.* the beam traverses 2.25 m of air, filled with an axial homogeneous magnetic field of 2 $Tesla$ strength out to a radius of 1.7 m, before reaching the calorimeter. Thus, this study covers the relevant range for the scintillator-tile calorimeter design which sees at 90° a coil equivalent to 9.54 cm of aluminium[12] and a shell of 1/8 $inch$ steel, corresponding to a total of 1.25 radiation lengths, and

possibly around half a radiation length from the tracking system in front of its sensitive region; at about 26°, near the barrel-endcap transition, these numbers increase to 2.86 plus about 1 radiation lengths. There is, in some designs for the electromagnetic section, a gap of about 8 cm between the barrel and the endcap, corresponding to $\Delta\eta \approx 0.04$. Requiring full shower containment, the gap effectively doubles leaving me with full shower acceptance over 96% of the rapidity range $|\eta| \leq 2.5$. To study the impact of the nonvertical angle of incidence on the resolution, I perform calculations with the 1.25 radiation lengths thick coil I have used before[5] at a few polar angles from 90° down to 30°. (This means stopping just short of the gap between the barrel and endcap because the gap is different in my model from the one in the current baseline design.) I do not include a tracking system model because that system will supposedly deliver the reference energies for measuring the correction *in situ*.

In the present study, I let ANLSIM and GEANT follow all particles in analog mode down to kinetic energies of 100 keV except photons which are taken down to 10 keV. Point deposits of energy created during the analog shower propagation are smeared with gamma distributions $\gamma(x; k, 1.0)$, with a variance of $k = 0.15^2\ GeV/E_{deposit}$, to give the overall simulation a consistent resolution behavior. The choice of γ distributions avoids the large negative tail of the smeared distribution of deposited energy which appear for a Gaussian of the same variance at the small energies of the deposits I have to deal with; the accumulated distributions for showers in the GeV energy range receive proper Gaussian-like shapes in this approach. For $\gamma(x; k, 1.0)$ distributions, the variance is equal to the mean, k. The algorithms for random number generation are taken from the Review of Particle Properties book[13] and a paper by Ahrens and Dieter.[14] The values of k requested by the simulation fall mostly into the interval $k = 10^{-3} - 10^{-1}$, distributed nearly flat over $log_{10}\ k$ in the specified range. At $k = 10^{-3}$, about 95.5% of the integral of the $\gamma(x; k, 1.0)$ distribution is located at $x < 10^{-20}$. This property delivers effectively a simulation of the sampling fraction of the calorimeter, rendering this technique appropriate for the present purpose. By comparing

program runs done at different times during the evolution of the present study, I find an uncertainty arising from the particular implementation of the gamma distributions in the measurement of the mean energy over the full event samples of about 1% which is much more than the statistical error of that mean. The resolutions receive from the same source an uncertainty of about 8% (relative).

The massless gap is chosen to be approximately the first radiation length of the active calorimeter, *i.e.* 8 mm in the coded detector out of a radial thickness of active calorimetry at 90° of 200.0 cm. This is the only type of longitudinal segmentation I use. Due to the approximation of having a continuous, totally active calorimeter, this corresponds most closely to a design in which a scintillator layer in front of the first absorber layer and a scintillator right behind the first absorber layer are both read out together. The transverse segmentation is a standard one, about $0.05 \cdot 0.05$ in the (η, ϕ) plane. I form clusters using seed cells containing at least 1 GeV of energy and collect all cells with more than 3 MeV (!) within a radius of $R = 0.5$ in the (η, ϕ) plane. If more than one cluster is found, I look only at the most energetic one. This choice eliminates all backscattered secondary particles that hit the calorimeter far away from the primary electron; obvious examples are contained in Fig.1.

Calling the signal from the first radiation length E_{front}, and the signal from the remainder of the calorimeter E_{back}, I write the measured energy

$$E_{corr} \;=\; \alpha_{mg} \cdot E_{front} \;+\; E_{back} \tag{2.1}$$

as has been used in refs.6-8. This equation can be inverted as

$$\alpha_{mg} \;=\; (E_{corr} - E_{back}) \;/\; E_{front} \tag{2.2}$$

if the correct energy E_{corr} is known. I use the measured mean energy from the program runs without any coil for this purpose, and calculate the correction factor on an event-by-event basis instead of from the mean values over all simulated

events. This allows me to measure the effect of fluctuations on the correction factor and the dependences both on the signal of the massless gap and the beam energy.

By design, the simulation represents a realistic data taking procedure, and the subsequent analysis is without modification suitable for application to an experimental approach of *measuring* the massless-gap correction; the desired nominal energy would there be supplied to sufficient accuracy by a magnetic measurement of the particle momentum. For electrons, even a measurement in the SSC interaction region is conceivable by selecting a sample of events containing clean decays $Z^0 \rightarrow e^+e^-$ as long as the resolution of the tracking system is noticeably better than the calorimeter resolution: The electrons can be defined by matching charged tracks with electromagnetic clusters without being limited severely by their relative and absolute inaccuracy, with the additional condition of having an e^+e^- pair near the Z^0 mass. Then the central detector will deliver a measurement of the desired energy E_{corr}, and a suitably designed calorimeter with a massless gap will provide the other two data elements, E_{front} and E_{back}. In the case of the SDC detector, the expected resolution of the tracking system[1] of $\sigma_{p_t}/p_t = 0.25\ (TeV/c)^{-1} \cdot p_t$ is fairly limited as at a momentum of 75 GeV/c at 90° one has only $\sigma_p/p \approx \sigma_E/E \approx 1.8\%$. This *in situ* determination will therefore work in the SDC detector only for energies below about 50 GeV (or less), *i.e.* a quite limited range in pseudorapidity and transverse momentum.

3. Analysis and results

I generate 500 events for every beam energy and coil thickness, except at 50 GeV where I have about 450 to 460 events each. For my reference case, the calorimeter model without any material in front of it (except for the 2.25 m of air), the mean energy response turns out to be very well linear. The resolution of $\sigma_E/E = 0.15/\sqrt{E}$ I have used to fluctuate the individual energy deposits is maintained in the total signal; this choice matches the expectation from experi-

mental data (Fig.2). The case without passive material provides for a good cross check for the determination of the correction factor α_{mg}: As there is nothing to correct for, it has to come out as $\alpha_{mg} = 1.0$ on average, and the fluctuations in its determination event-by-event reflect the fluctuations in the energy measurements in the front and back sections with a variance of

$$\begin{aligned}(\sigma_\alpha)^2 &= \frac{(\alpha_{mg}\sigma_{front})^2 + (\sigma_{back})^2}{E^2{}_{front}} \\ &\approx \left(\frac{\sigma_{back}}{E_{front}}\right)^2 \quad \text{for } \sigma_{back} \gg \sigma_{front}\end{aligned} \tag{3.1}$$

(derived from eq.(2.2)). Taking as an example the mean and r.m.s. values for electrons at 20 GeV/c,

$$\begin{aligned}E_{corr} &= 19.95\ GeV \\ E_{back} &= 19.91\ GeV \\ E_{front} &= 0.0264\ GeV \\ \sigma_{back} &= 0.715\ GeV \\ \sigma_{front} &= 0.0275\ GeV \\ <\alpha_{mg}> &= 1.50 \quad ,\end{aligned}$$

I obtain

$$\sigma_\alpha \approx 27.1 \quad , \tag{3.2}$$

almost independent of α_{mg}, from eq.(3.1) which compares very well to the actual distribution of the correction factors measured in the simulation run (Fig.3; this is true also for the other energies investigated). With the statistics available, the expected "measurement" error for the mean $\alpha_{mg} = 1.0$ is $\Delta\alpha_{mg} \approx 1.2$. This sets the scale at which I can claim significance for the need of a correction.

Considering now material in front of the calorimeter, in totals of one, two, three and five radiation lengths of aluminimum in a coil arrangement (Fig.1), I find a clear peak developing in the distribution of the correction factor α_{mg}, with

a part of the long tails from the shower fluctuations still present in the case of only one radiation length of material (Fig.3). The mean value of the peak is a few for the larger amounts of material, in agreement with the results previously obtained[7] for the SDC liquid argon calorimeter design. These "well-defined" correction factors appear actually as soon as the detected energy in the massless gap exceeds the average size it has with no material in front. This becomes obvious in the scatterplots of α_{mg} versus the energy E_{front} as well as versus the ratio E_{front}/E_{back} (Figs.4,5). At this point, a possible choice for performing a correction is to use the mean value of the event-by-event determined factors (Tab.1)* . This improves the raw resolutions (for more than one radiation length of passive material) already quite significantly (Tab.2, second column). Picking by hand some near-average values independent of the beam energy I can retain most of the improvement. This means that increasing the signal output from the massless gap by those energy-independent factors for the appropriate amount of passive material in front, this part of the best possible correction can be built into the detector, leaving a smaller correction to be done by software afterwards. For only one radiation length of passive material in front of the calorimeter, the deterioration effects are small; correspondingly the corrections are still quite badly defined and do not deliver any noticeable improvement. All of this agrees well with the recent study done by Barry Wicklund.[9]

With the good statistics I have available, I go one step further and look at a correlation between α_{mg} and the gap energy or energy ratio. By averaging the α_{mg} values for small bins of the gap energy or energy ratio, I find a clear dependence of the best correction factor on the energy observed in the massless gap (Figs.6,7) for the larger amounts of passive material. I fit these distributions

* Actually, the means are determined by fitting Gaussian curves to the central parts of the distributions. The resulting factors are mostly only a little smaller than the directly calculable unrestricted means of the distributions. They are better determined in all cases and exhibit a more reasonable variation with energy and the thickness of passive material. The resulting resolutions do not deviate much from those obtained with the unrestricted means. In particular, the unrestricted means do *not* fully restore the linearity of the calorimeter response, a topic discussed further below.

with an exponential function plus a constant. Comparing the use of the front energy or the front-to-back ratio as a parameter, I observe here that the front energy seems to give a little better defined functions than the ratio and choose therefore to use the front energy as a parameter for the determination of all my corrections. Applying these functions does not improve the resolutions noticeably over the constant factor corrected results. This is likely due to the still limited statistics in particular for the smallest signals from the massless gap. In some cases, foremost the angular dependence at 50 GeV, a sensible determination of such functions is even impossible.

To have a useful correction function for the final experiment, I need to interpolate between the chosen energies where I have determined the correction. For this purpose, I look at the dependence of the coefficients both on the energy and the thickness of the passive material with the added boundary condition that $\alpha_{mg} \rightarrow 1.0$ in either limit of high particle energy and vanishing material thickness. The following parametrization

$$\begin{aligned} \alpha_{mg}(d,E) &= 1.0 \; + \; a_1 \cdot d \; + \; a_2 \cdot e^{-a_3 \cdot E} \\ a_1 &= 0.7729 \\ a_2 &= 3.888 \\ a_3 &= 0.14435 \end{aligned} \tag{3.3}$$

with d being the thickness of the passive material in units of radiation length, X_0, and E the incident energy in GeV, turns out to give a good final result, not optimized but as good as, and in the angular dependence for the SDC coil even better than, the correction with the constant factors (Tab.2). The coefficients a_i are determined from crudely fitting the individual factors in the table with the function of eq.(3.3). For nonvertical angles of incidence, I take out the $1/sin\theta$ facotr of increase in the thickness of the massless gap effect by multiplication,

$$\alpha_{mg}(\theta) \; = \; \alpha_{mg}(90^\circ) \cdot sin\theta \quad .$$

(Note that the geometry as chosen here gives a signal enhancement just due to

this factor as a constant thickness of the massless gap *transversely to the beam axis* is assumed.) The passive material thickness still has to be taken along the direction of the incident electron, not transversely to the beam. The resulting resolutions are shown in Fig.8. (The previously noted uncertainties inherent in the simulation are responsible for the scattering of the points.)

Beyond the deterioration of the resolution, I also have to look at the behavior of the mean response (Tab.3). Although in first approximation the reduced response is "calibrated away", such a calibration is an expression of the mere fact that the passive material in front of the calorimeter gives rise to a nonlinearity in the response in an energy region of high importance for achieving the physics goals of the SDC experiment, *e.g.* the measurements of the masses of the Z^0, or through it of the neutral Higgs boson, or of the top quark using pairs of an isolated electron with a nonisolated muon.[1] (Remember that, as mentioned before, at energies beyond about 50 GeV the tracking system will not any more outperform the calorimeter on resolution.) On this front I find that the corrections do in fact reduce also the nonlinearity significantly, with the overall funtional correction again giving the best results. As a bottom line both on the resolution and the linearity issues, for the amounts of passive material to be dealt with in the scintillator-tile calorimeter of SDC, the corrections from a massless gap are fairly small at the center of the barrel calorimeter (compared to *e.g.* a liquid argon calorimeter[6-8]), increasing somewhat towards the endcap regions due to the $1/sin\theta$ effect. A constant enhancement factor along the barrel, independent of energy, does already improve both the resolution and linearity although without removing the need for further corrections to be done after data taking. On this basis, an extensive study of the final calorimeter design will be needed to establish the particular technique of setting up a massless gap. This is beyond the scope of the present work.

4. Summary

I have studied a massless gap approach to correcting the calorimeter response to electromagnetic showers for passive material in front of the calorimeter. I find that at two radiation lengths of passive material, the correction using this approach becomes worthwhile, delivering a noticeable improvement. A part of the correction can be built into the detector by designing for an appropriately enhanced signal from the massless gap. Beyond the recovery of the resolution, the nonlinearity introduced by the passive material is also noticeably eased.

ACKNOWLEDGEMENTS

I gratefully acknowledge the interest and contributions of Dr. Tom Kirk who not only brought the whole issue to my attention, thereby initiating this study, but also supported its development throughout with his comments, suggestions and criticism. I also thank Dr. Chris Hearty for his opinions and ideas, and Dr. David Malon for his support and consulting in getting a handle on the gamma distributions for my programs.

REFERENCES

1) Solenoid Detector Collaboration, G.H.Trilling et al., SDC-90-00085 and SSC-EOI-3, SSC Laboratory, Dallas, Texas, May 24, 1990, and SDC-90-00151 and SSC-LOI-1, SSC Laboratory, Dallas, Texas, November 30, 1990

2) A.M.Jonckheere, Simulating D0 and Hermeticity Studies or How to Effect a Detector Design, Proc. Workshop on Detector Simulation for the SSC, August 24-28, 1987, ed. L.E.Price, ANL-HEP-CP-88-51, Argonne National Laboratory, Argonne, Illinois, USA 1988, p.270, p.175

3) M.Strovink, W.J.Womersley and G.E.Forden, Hermeticity of three Cryogenic Calorimeter Geometries, Proceedings of the Workshop on Calorimetry for the Supercollider, March 13-17, 1989, Tuscaloosa, Alabama, U.S.A., eds. R.Donaldson and M.D.G.Gilchriese, World Scientific Publishing Co. Pte. Ltd., Singapore, 1990, p.9

4) R.Ruchti, Summary Report for the Scintillating Fiber Working Group, Proceedings of the Workshop on Tracking Systems for the Superconducting Supercollider, July 24-28, 1989, TRIUMF Laboratory, Vancouver, Canada, 1989, E3

5) T.B.W.Kirk and H.-J.Trost, The effect of passive material on the detection of hadrons in calorimeter configurations for the SDC detector, ANL/HEP/TR-91/62 and SDC-91-00050

6) H.Hirayama, Effects of dead material to the electro-magnetic calorimeter and energy/resolution recovery with "massless gap", JSD-NOTE-1990-30 and SDC-90-00108, Nucl.Instr.Meth. A302 (1991) 427

7) Ch.Hearty, Resolution and hermeticity of the liquid argon electromagnetic calorimeter as a function of pseudorapidity, SDC-90-00145-REV

8) SDC Liquid Argon Group, Calorimeter conceptual design - liquid argon option, 5 August 1991 (uncatalogued)

9) A.B.Wicklund, EGS4 studies of CDF preshower response: B-field effects and "massless gap" resolution response, CDF/ANAL/ELECTRON /PUB/1639, 2 January 1992

10) R.E.Blair, L.E.Price and H.-J.Trost, program ANLSIM, Argonne National Laboratory, Argonne, Illinois, USA 1989, version 1.05, 1991 (unpublished);
H.-J.Trost, ANLSIM, talk given at: Workshop on the Future Development of GEANT, SSC Laboratory, Dallas, Texas, Jan.10-13, 1990, unpublished;
R.E.Blair, The Argonne National Laboratory Simulation Package, Proceedings of the Workshop of Physics and Detector Simulation for SSC Experiments, SSC Laboratory, Dallas, Texas, January 9-19, 1990, vol.1, p.69;
H.-J.Trost, How to Use ANLSIM, ibid., vol.2, p.265

11) J.Proudfoot and H.-J.Trost, A first simulation study of the barrel-endcap transition region in a calorimeter of the scintillator tile design, ANL-HEP-TR-90-77 and SDC-90-00073

12) R.Fast *et al.*, SDC Calorimeter Group Meeting at Fermilab, May 21-22, 1991

13) Particle Data Group, Review of Particle Properties, Phys.Lett. 239B (1990), p.III.38, algorithm for $k > 1$; note that for the second parameter not equals to 1.0 as well as for $k < 1$, the algorithms don't work as given there.

14) J.H.Ahrens and U.Dieter, Computing 12 (1974) 223, algorithm GS for $k < 1$

TABLE CAPTIONS

1. Correction factors: individual mean factors, energy independent factors

2. Resolutions for different massless gap correction schemes: no correction, individual mean, energy independent mean, individual function, overall function

3. Mean responses for different massless gap correction schemes: no correction, individual mean, energy independent mean, individual function, overall function

FIGURE CAPTIONS

1. Calorimeter and coil model (2 X_0 version) used in ANLSIM for the present study. The shower included is due to an electron of 20 GeV/c momentum (the same event in the overview and the enlarged view), and particle trajectories are shown for kinetic energies beyond 10 MeV.

2. Mean response and resolution over incident energy for electrons in the simulated calorimeter

3. Event-by-event determined correction factor α_{mg} for electrons with a momentum of 20 GeV/c, a) with no passive material in front of the calorimeter, b) with 1 X_0 of aluminium in front, c) with 2 X_0, d) with 3 X_0, e) with 5 X_0. The distributions are fit with a single Gaussian in the range $\alpha_{mg} = -25.0 \rightarrow +25.0$.

4. Distribution of α_{mg} versus the detected gap energy E_{front}, for electrons at 20 GeV/c; cases as in Fig.3

5. Distribution of α_{mg} versus the ratio of energies E_{front}/E_{back}, for electrons at 20 GeV/c; cases as in Fig.3

6. Dependence of α_{mg} on the gap energy E_{front}, for electrons at 20 GeV/c; cases as in Fig.3

7. Dependence of α_{mg} on the energy ratio E_{front}/E_{back}, for electrons at 20 GeV/c; cases as in Fig.3

8. Resolution dependence on a) the thickness of passive material and b) the angle of incidence into the coil and calorimeter

Table 1*a* : Mean correction factors for different electron energies and thicknesses of passive material

	10 *GeV*	20 *GeV*	50 *GeV*	energy independent
0 X_0	-0.1755	1.502	-1.096	1.0
1 X_0	2.638	0.1564	0.3843	1.1
2 X_0	3.006	2.337	1.913	2.2
3 X_0	4.408	3.595	3.127	3.3
5 X_0	6.381	5.510	4.491	5.5

Table 1*b* : Mean correction factors for different electron energies and angles of incidence into the SDC coil

	10 *GeV*	20 *GeV*	50 *GeV*	energy independent
90°	1.018	1.101	1.089	1.4
45°	1.230	1.266	1.122	1.4
35°	1.255	1.231	1.033	1.4
30°	1.292	1.239	0.9787	1.4

The correction factor is changed to 1.0 for 0 X_0 always (nothing to correct) and for $\alpha_{mg} < 1.0$ (values less than 1.0 do not make sense, and their errors are still larger than 1.0).

Table 2a : Resolutions (in GeV) for different massless-gap correction schemes: Dependence on thickness of passive material

	no correction	individual mean	individual function	energy independent	overall function
10 GeV					
0 X_0	0.4975				
1 X_0	0.4633	0.4882	0.4803	0.4656	0.4867
2 X_0	0.5356	0.5296	0.5291	0.5280	0.5618
3 X_0	0.6322	0.6366	0.6131	0.5904	0.6313
5 X_0	0.9567	0.8978	0.9826	0.8912	0.8876
20 GeV					
0 X_0	0.6790				
1 X_0	0.7001	(0.7001)	0.6834	0.7008	0.6997
2 X_0	0.7591	0.7539	0.7537	0.7546	0.7473
3 X_0	0.9960	0.8746	0.9092	0.8743	0.8799
5 X_0	1.261	1.132	1.132	1.134	1.079
50 GeV					
0 X_0	1.032				
1 X_0	1.144	(1.144)	(1.144)	1.137	1.138
2 X_0	1.229	1.156	1.145	1.152	1.130
3 X_0	1.582	1.281	1.392	1.313	1.314
5 X_0	2.415	1.705	1.812	1.734	1.708

For values in parentheses, no sensible correction could be determined and therefore none was applied (i.e. the factor was set to 1.0 flat).

Table 2b : Resolutions (in GeV) for different massless-gap correction schemes: Dependence on angle of incidence

	no correction	individual mean	individual function	energy independent	overall function
10 GeV					
90°	0.4711	0.4725	0.4867	0.4556	0.4780
45°	0.4926	0.4768	0.4862	0.4724	0.4842
35°	0.5544	0.5475	0.5595	0.5474	0.5576
30°	0.5941	0.5776	0.6024	0.5733	0.5436
20 GeV					
90°	0.6990	0.6943	0.7232	0.7029	0.6996
45°	0.6728	0.6739	0.6884	0.6537	0.6784
35°	0.7266	0.7272	0.7455	0.7046	0.7101
30°	0.8235	0.7618	0.8279	0.7561	0.7254
50 GeV					
90°	1.067	1.064	N/A	1.057	1.084
45°	1.108	1.101	N/A	1.067	1.073
35°	1.207	1.213	N/A	1.235	1.217
30°	1.311	(1.311)	N/A	1.211	1.180

For values in parentheses, no sensible correction could be determined and therefore none was applied (i.e. the factor was set to 1.0 flat). At 50 GeV, no reasonable individual fits were obtained.

Table 3 : Responses (in GeV) for different massless-gap correction schemes: Dependence on thickness of passive material

	no correction	individual mean	individual function	energy independent	overall function
10 GeV					
0 X_0	10.01				
1 X_0	9.845	9.991	9.904	9.850	9.995
2 X_0	9.430	9.869	9.801	9.694	9.962
3 X_0	8.662	9.767	9.692	9.393	9.727
5 X_0	7.351	9.621	9.622	9.248	9.334
20 GeV					
0 X_0	19.95				
1 X_0	19.83	(19.83)	19.71	19.84	19.94
2 X_0	19.26	19.66	19.66	19.61	19.80
3 X_0	18.02	19.39	19.52	19.23	19.37
5 X_0	16.12	19.33	19.33	19.33	18.98
50 GeV					
0 X_0	49.90				
1 X_0	49.78	(49.78)	(49.78)	49.81	49.90
2 X_0	49.02	49.44	49.39	49.59	49.76
3 X_0	47.17	49.07	48.99	49.23	49.26
5 X_0	43.91	48.64	48.78	50.02	49.14

For values in parentheses, no sensible correction could be determined and therefore none was applied (i.e. the factor was set to 1.0 flat).

Table 3 : Responses (in GeV) for different massless-gap correction schemes: Dependence on angle of incidence

	no correction	individual mean	individual function	energy independent	overall function
10 GeV					
90°	9.781	9.784	9.825	9.830	10.00
45°	9.534	9.605	9.590	9.659	9.970
35°	9.200	9.339	9.330	9.430	9.825
30°	8.904	9.153	9.123	9.233	9.666
20 GeV					
90°	19.78	19.78	19.60	19.83	19.94
45°	19.40	19.49	19.48	19.55	19.75
35°	18.94	19.14	19.10	19.27	19.50
30°	18.47	18.76	18.81	18.99	19.20
50 GeV					
90°	49.67	49.69	N/A	49.76	49.88
45°	49.11	49.19	N/A	49.38	49.58
35°	48.46	48.50	N/A	49.00	49.17
30°	47.78	(47.78)	N/A	48.62	48.80

For values in parentheses, no sensible correction could be determined and therefore none was applied (i.e. the factor was set to 1.0 flat). At 50 GeV, no reasonable individual fits were obtained.

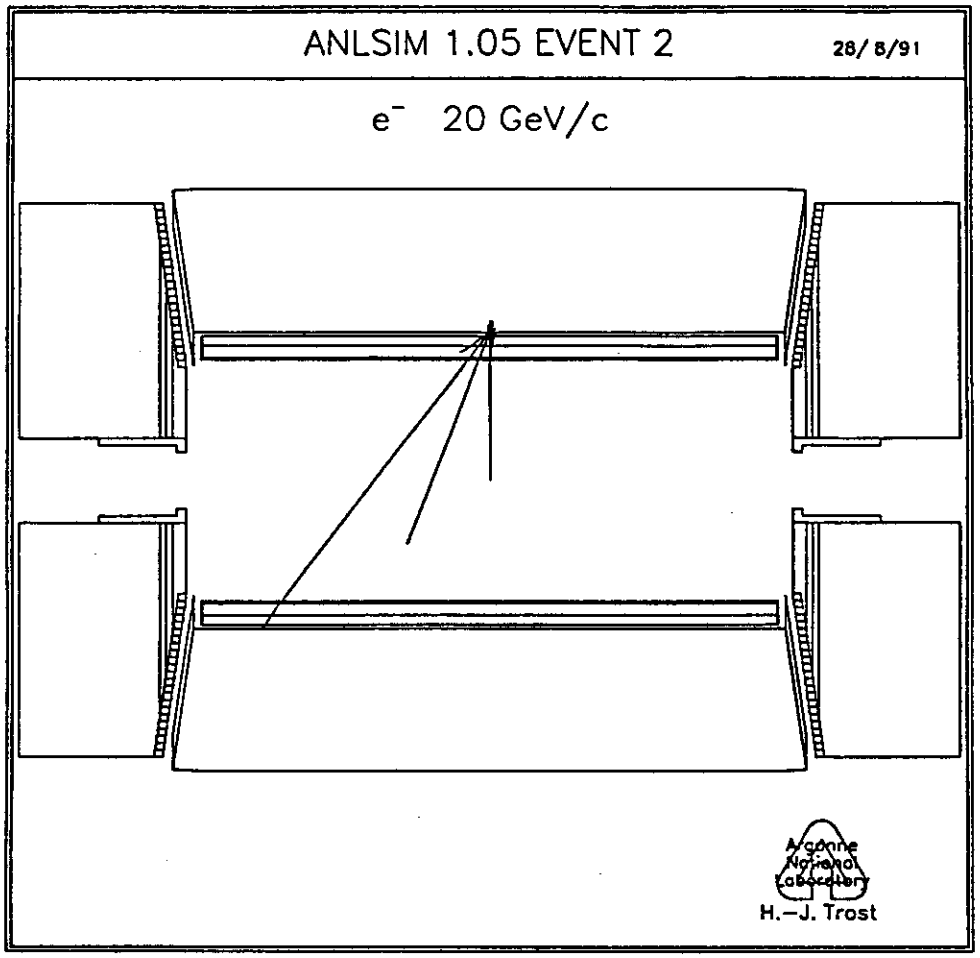
ANLSIM 1.05 EVENT 2
28/8/91
e⁻ 20 GeV/c
Argonne National Laboratory
H.-J. Trost

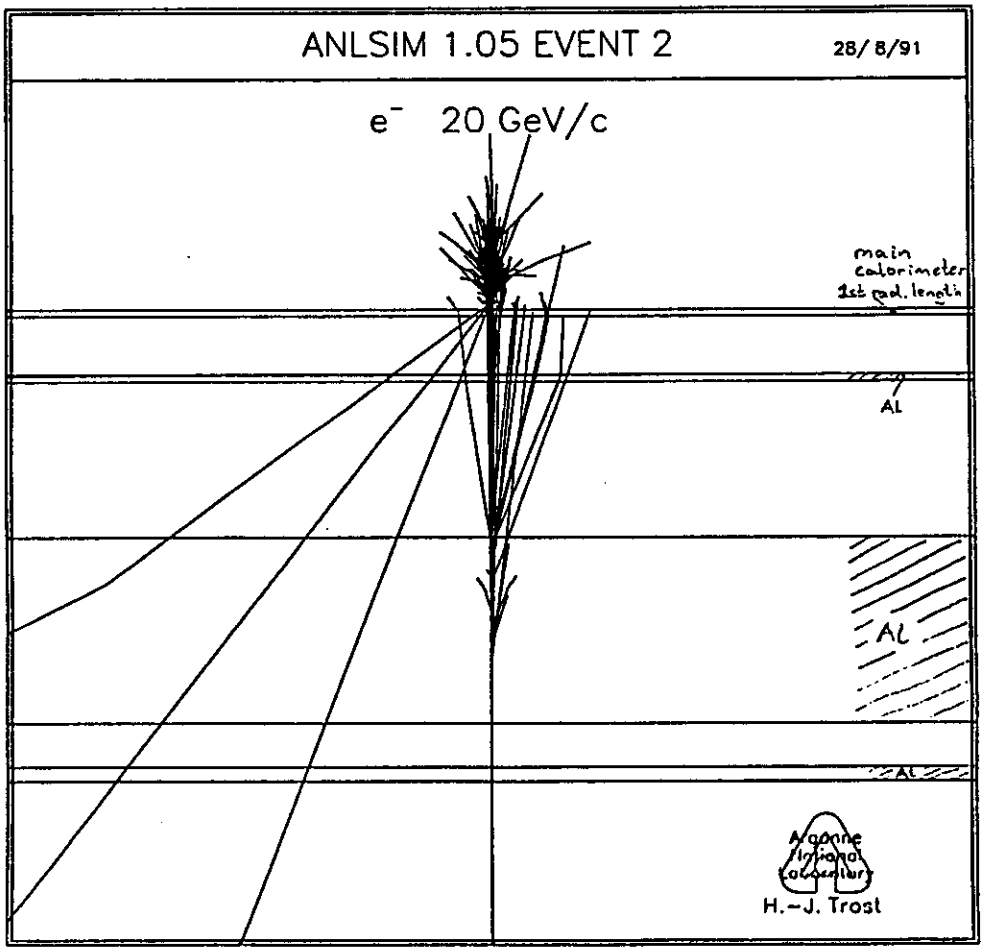
ANLSIM 1.05 EVENT 2
28/8/91
e⁻ 20 GeV/c
main calorimeter
1st rad. length
AL
AL
AL
Argonne National Laboratory
H.-J. Trost

Fig.1

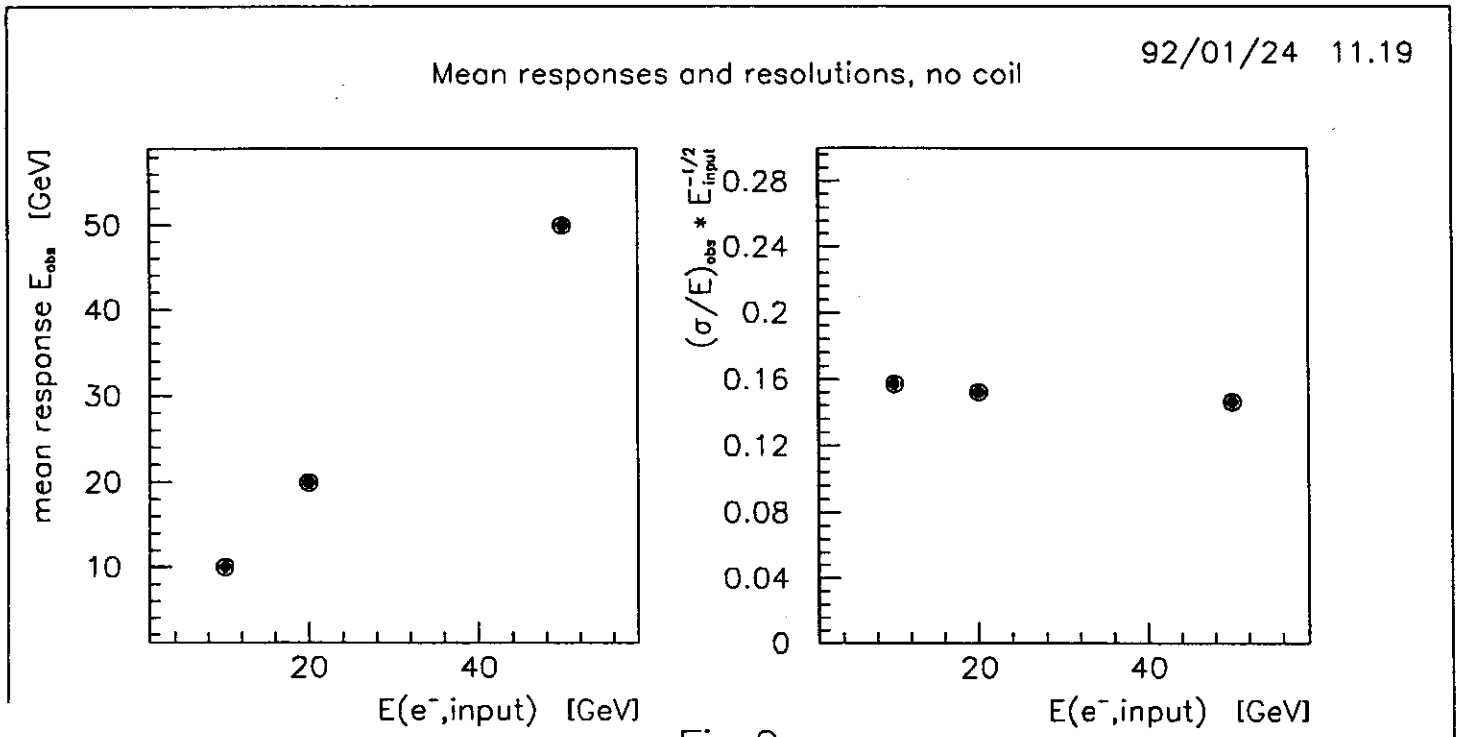
92/01/24 11.19
Mean responses and resolutions, no coil
mean response E_{obs} [GeV]
50
40
30
20
10
20
40
E(e⁻,input) [GeV]
$(\sigma/E)_{obs} * E_{input}^{-1/2}$
0.28
0.24
0.2
0.16
0.12
0.08
0.04
0
20
40
E(e⁻,input) [GeV]

Fig.2

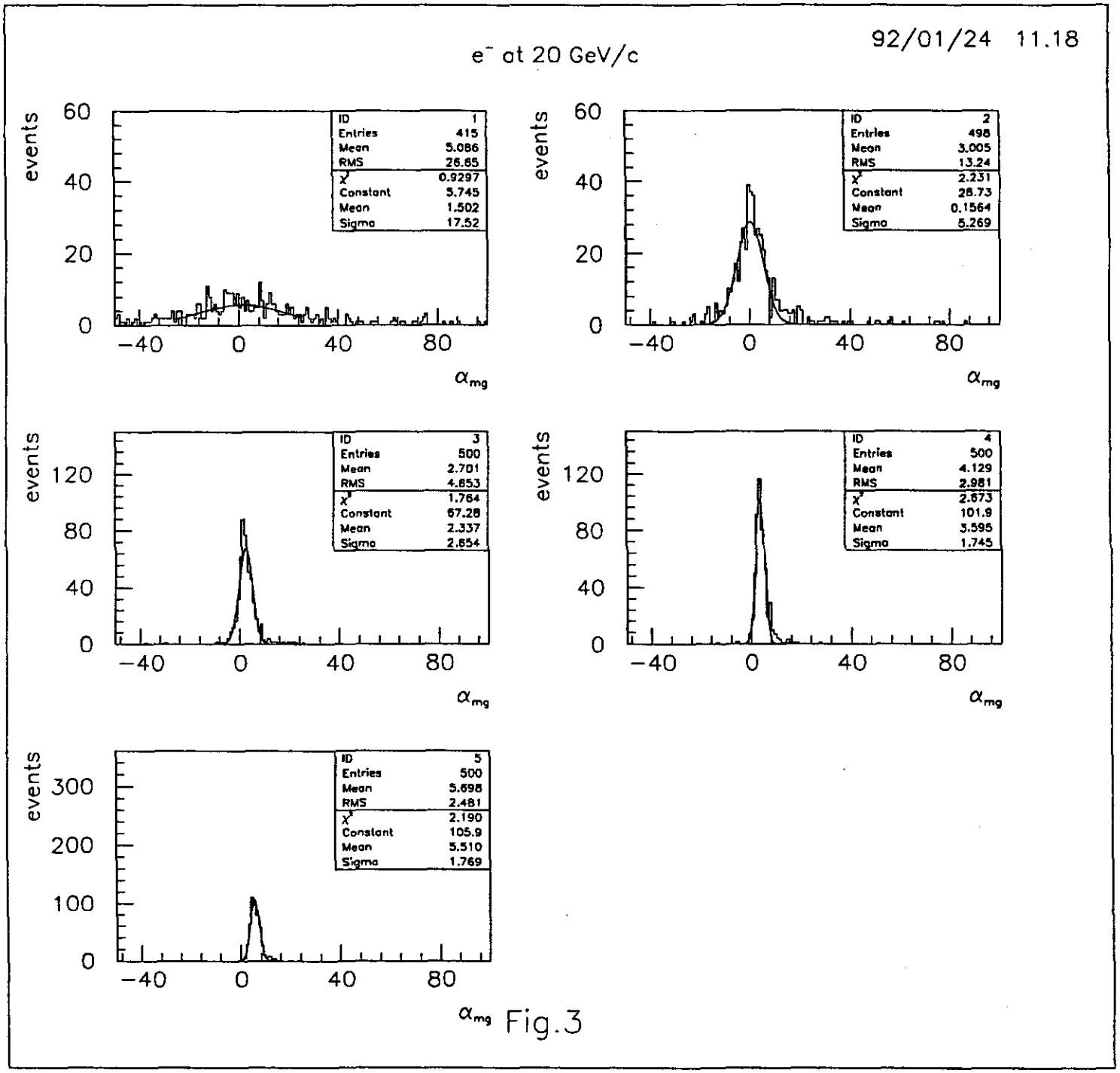
92/01/24 11.18
e⁻ at 20 GeV/c
events
α_{mg}
ID 1
Entries 415
Mean 5.086
RMS 26.65
χ² 0.9297
Constant 5.745
Mean 1.502
Sigma 17.52
ID 2
Entries 498
Mean 3.005
RMS 13.24
χ² 2.231
Constant 28.73
Mean 0.1564
Sigma 5.269
ID 3
Entries 500
Mean 2.701
RMS 4.653
χ² 1.764
Constant 67.28
Mean 2.337
Sigma 2.654
ID 4
Entries 500
Mean 4.129
RMS 2.981
χ² 2.673
Constant 101.9
Mean 3.595
Sigma 1.745
ID 5
Entries 500
Mean 5.698
RMS 2.481
χ² 2.190
Constant 105.9
Mean 5.510
Sigma 1.769

Fig.3

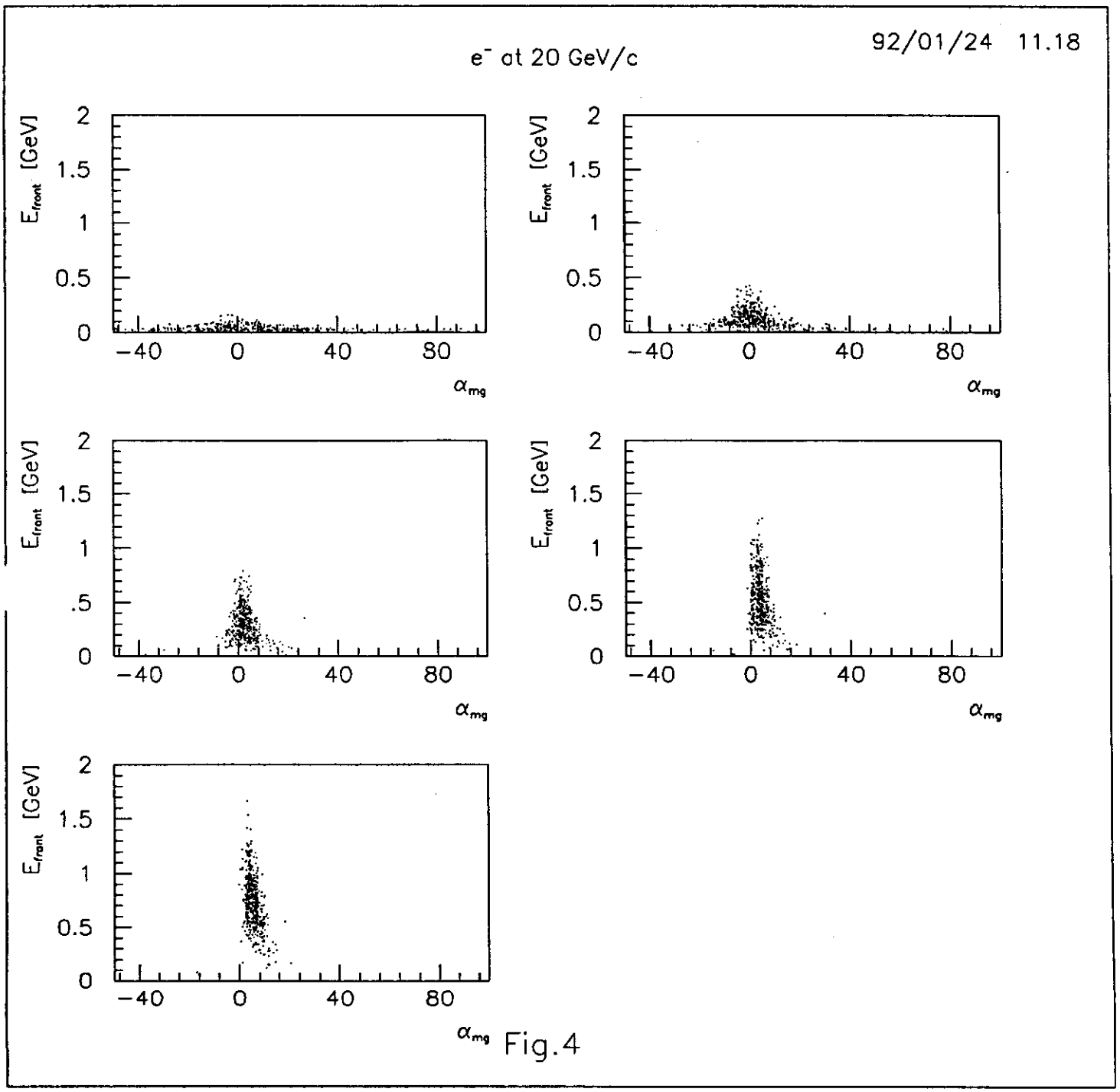

Fig.4

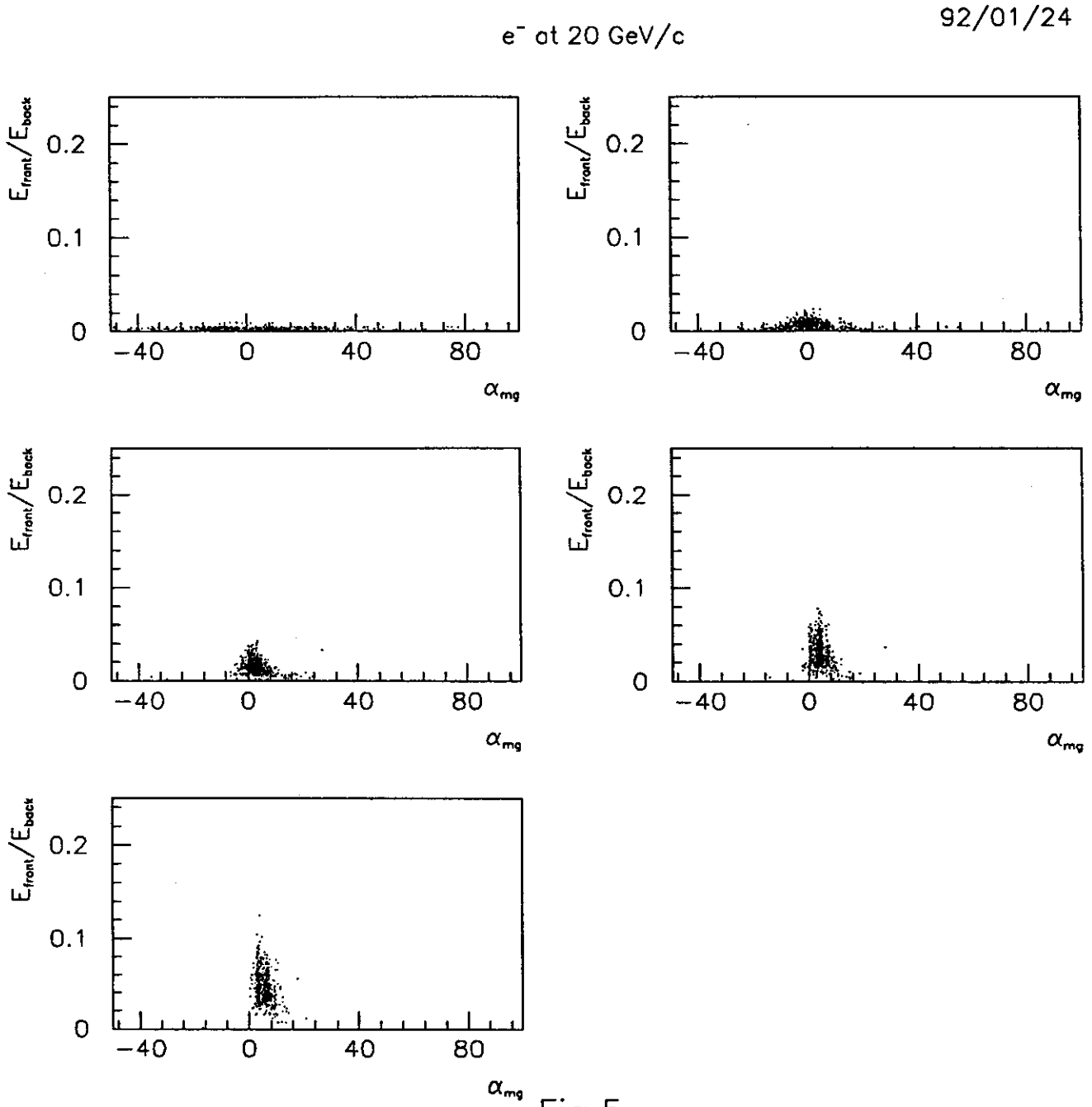

Fig.5

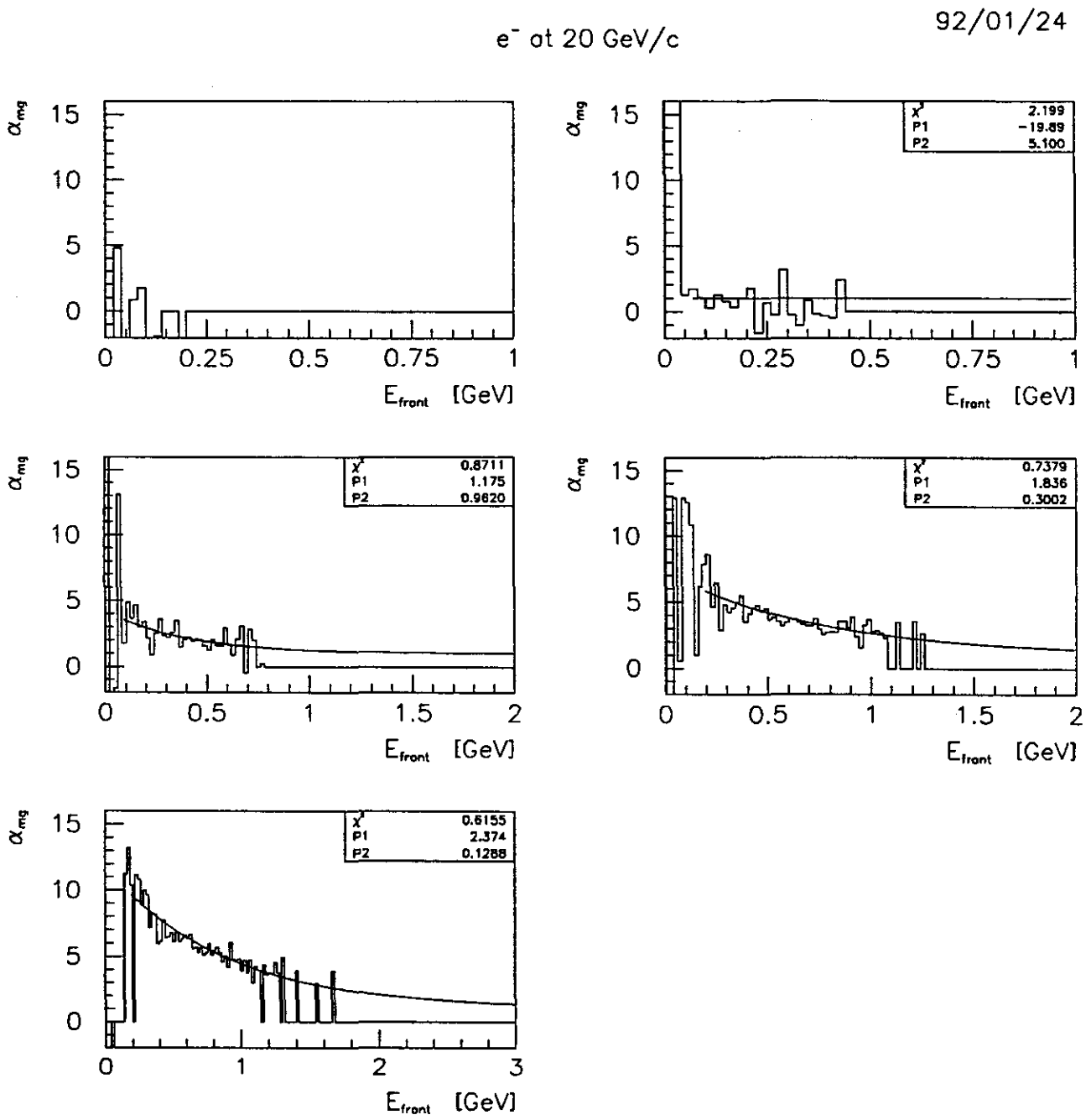
92/01/24 11.18
e⁻ at 20 GeV/c
α_{mg}
E_{front} [GeV]
χ^2 2.199
P1 -19.89
P2 5.100
χ^2 0.8711
P1 1.175
P2 0.9620
χ^2 0.7379
P1 1.836
P2 0.3002
χ^2 0.6155
P1 2.374
P2 0.1288

Fig.6

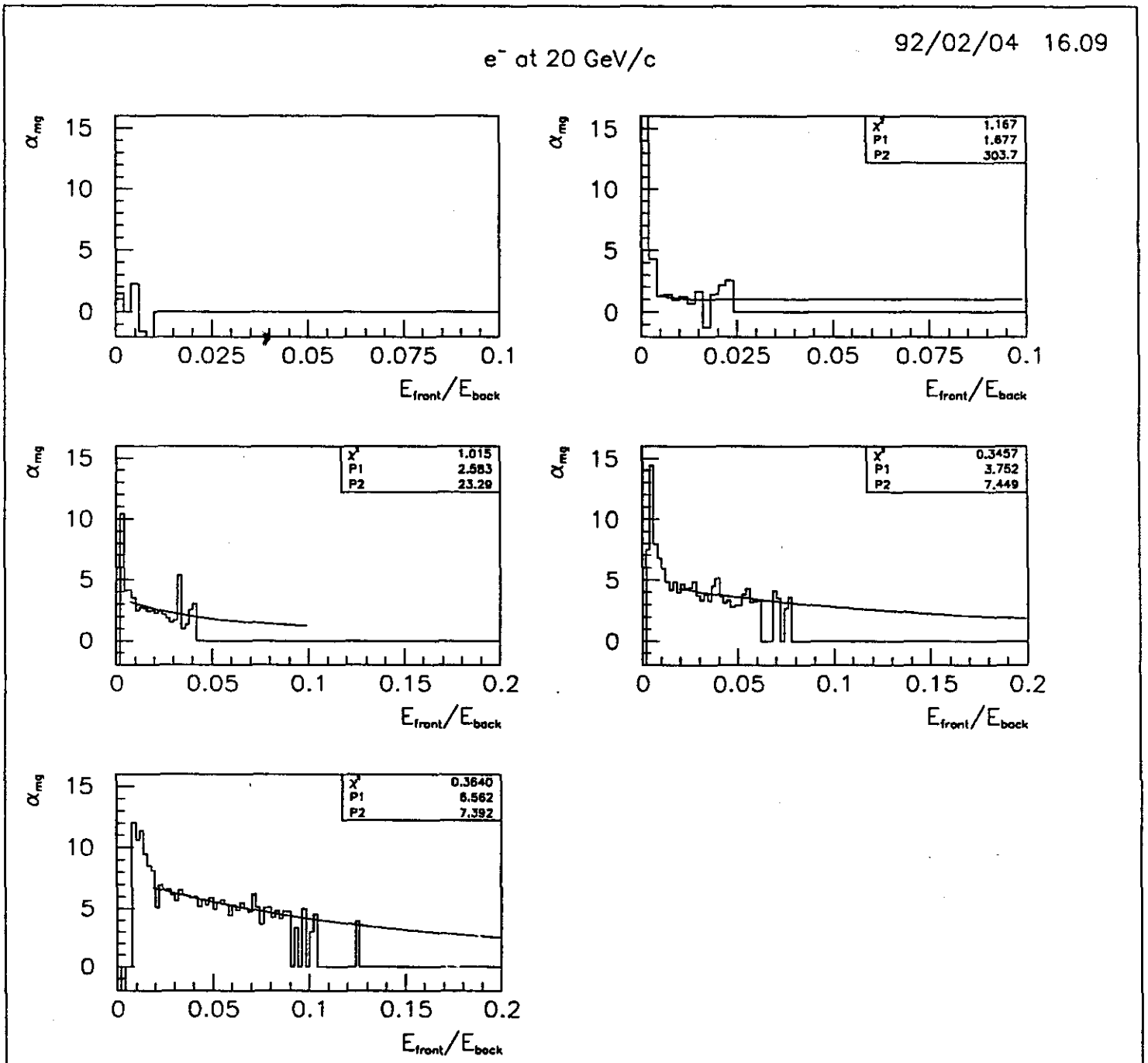
92/02/04 16.09
e⁻ at 20 GeV/c
α_{mg}
E_{front}/E_{back}
χ^2 1.167
P1 1.677
P2 303.7
χ^2 1.015
P1 2.583
P2 23.29
χ^2 0.3457
P1 3.752
P2 7.449
χ^2 0.3640
P1 6.562
P2 7.392

Fig.7

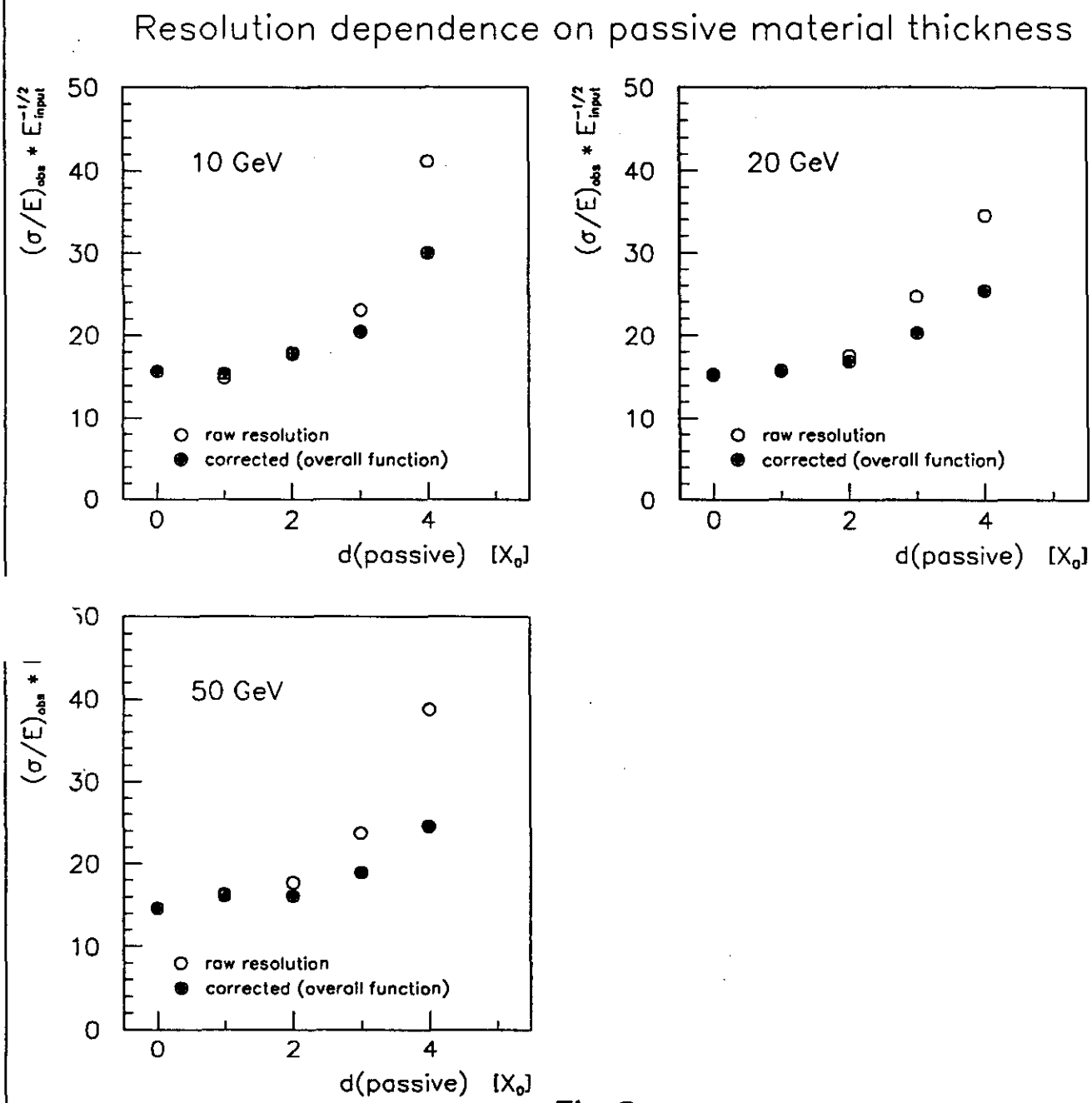
Resolution dependence on passive material thickness
10 GeV
20 GeV
50 GeV
$(\sigma/E)_{obs} * E_{input}^{-1/2}$
raw resolution
corrected (overall function)
d(passive) [X_0]
0
10
20
30
40
50
2
4

Fig.8a

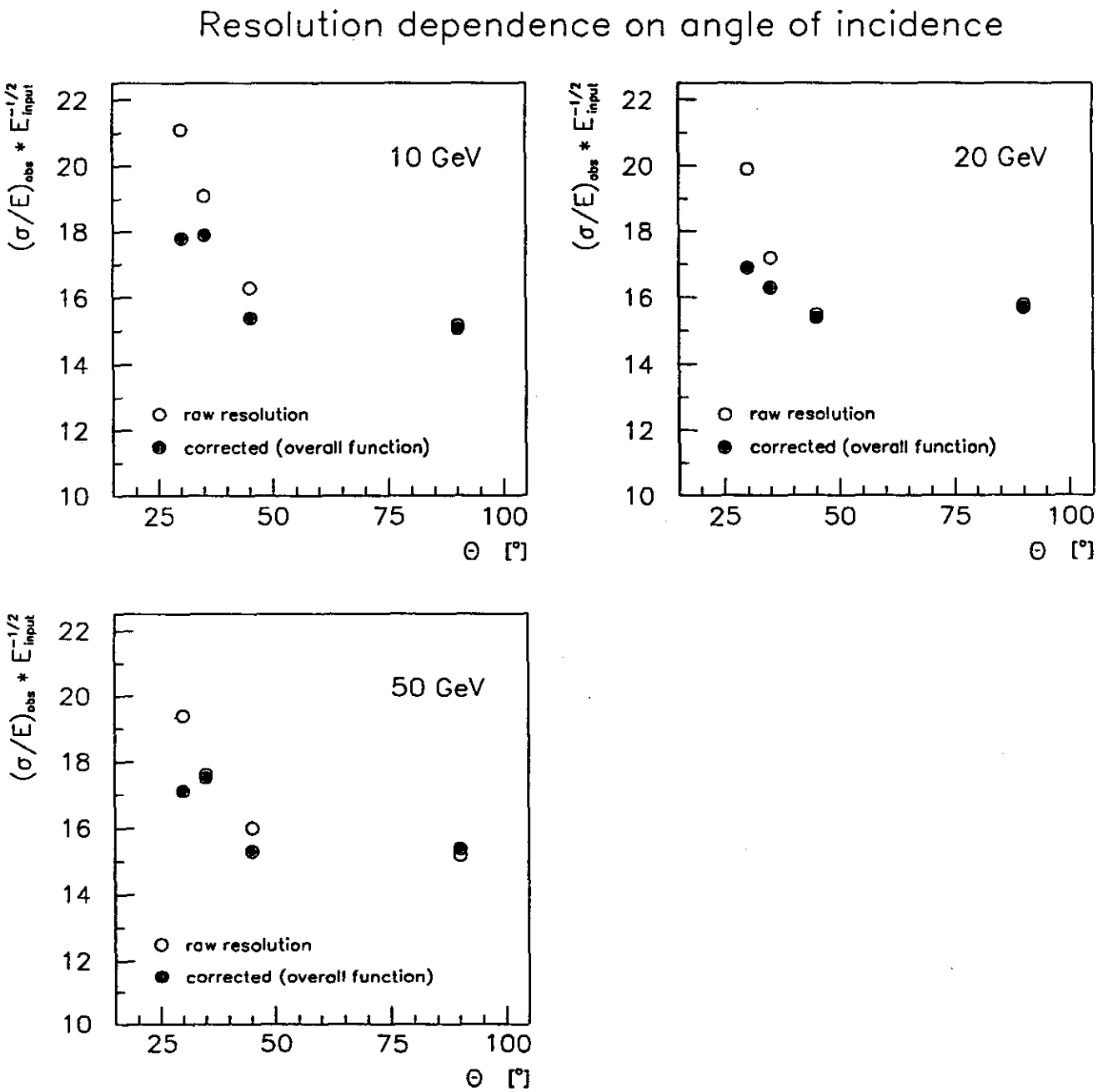
Resolution dependence on angle of incidence
$(\sigma/E)_{abs} * E_{input}^{-1/2}$
10 GeV
20 GeV
50 GeV
raw resolution
corrected (overall function)
Θ [°]
22
20
18
16
14
12
10
25
50
75
100

Fig.8b